



HHS Public Access

Author manuscript

Int J Pharm. Author manuscript; available in PMC 2015 December 21.

Published in final edited form as:

Int J Pharm. 2014 January 2; 460(0): 240–247. doi:10.1016/j.ijpharm.2013.11.007.

Dermal permeation of 2-hydroxypropyl acrylate, a model water-miscible compound: Effects of concentration, thermodynamic activity and skin hydration

H. Frederick Frasch^{a,*}, Ana M. Barbero^a, G. Scott Dotson^b, and Annette L. Bunge^c

^aHealth Effects Laboratory Division, National Institute for Occupational Safety and Health, Morgantown, WV 26505, USA

^bEducation and Information Division, National Institute for Occupational Safety and Health, Cincinnati, OH 45226, USA

^cChemical and Biological Engineering Department, Colorado School of Mines, Golden, CO 80401, USA

Abstract

The goal of these studies was to measure and interpret the skin permeability characteristics of 2-hydroxypropyl acrylate (HPA) as a model compound that is completely miscible with water.

Methods—*In vitro* permeation from HPA-H₂O binary mixtures through human epidermis and silicone membranes was measured. Thermodynamic activities of HPA and H₂O in these mixtures were determined. Permeation was also measured through epidermis and silicone from donor solutions with constant HPA activity but different H₂O activities. Water uptake into desiccated human stratum corneum (SC) equilibrated with HPA-H₂O mixtures was determined.

Results—Steady-state flux of HPA through silicone was a linear function of HPA activity but not HPA concentration. For epidermis on the other hand, flux increased with HPA activity only for HPA activities > 0.35. At constant HPA activity, flux decreased 4.5-fold as water activity decreased from 1 to 0.8. Incubation of SC with HPA-H₂O mixtures resulted in substantial changes in SC water content, dependent on the water activity of the mixture and consistent with measured SC water sorption data.

Conclusions—These experiments provide unequivocal evidence of a substantial increase in epidermal barrier function resulting from SC dehydration. Dehydration-related alterations in the SC appear responsible for the observed flux characteristics.

Keywords

Skin absorption; Lag time; Stratum corneum; Skin hydration; Acrylic monomers; Thermodynamic activity

*Corresponding author at: NIOSH, 1095 Willowdale Road, Morgantown, WV 26505, USA. Tel.: +1 304 285 5755; fax: +1 304 285 6041. H.Frasch@cdc.gov (H.F. Frasch).

Disclaimer

The findings and conclusions in this report have not been formally disseminated by the National Institute for Occupational Safety and Health (NIOSH) and should not be construed to represent any agency determination or policy.

1. Introduction

2-Hydroxypropyl acrylate (HPA, Table 1) is a monomer that is used primarily in thermosetting resins for surface coatings, adhesives, and textiles. HPA and water are miscible in all proportions at room temperature. Other chemicals with similarly high aqueous solubility display unusual skin permeation behavior. For example, the dermal permeation of 2-butoxyethanol (BE) in aqueous solutions has been a matter of debate based on the observation that steady-state dermal flux (J_{SS}) of BE is a strongly non-linear function of BE concentration (Johanson and Fernstrom, 1988; Traynor et al., 2007). Three distinct regions of behavior have been noted. At low concentrations, J_{SS} increases with increasing BE concentration. At intermediate concentrations, J_{SS} remains relatively constant, while at high concentrations, J_{SS} decreases with BE concentration to such an extent that flux from neat BE is about the same as from a 10 wt.% solution.

Bunge et al. (2012) have summarized these observations on BE and presented a reasonable explanation. They pointed out that the general driving force for permeation is thermodynamic activity, not concentration (Higuchi, 1960). Additionally, the thermodynamically appropriate metric for concentration is mole fraction and not volume fraction or weight fraction, which are typically used. For ideal solutions, thermodynamic activity is a linear function of mole fraction, but not, in general, of volume or weight fraction. Thus, for an ideal solution that does not alter the membrane barrier, J_{SS} is a linear function of the mole fraction of the chemical. BE-water forms a non-ideal solution. Therefore, the thermodynamic activity in aqueous BE solutions must be known in order to make informative observations on BE flux. Bunge et al. (2012) showed that activity-normalized BE fluxes are constant up to a weight fraction of about 0.8. For higher concentrations, a sharp drop in the activity-normalized flux corresponds to a sharp decrease in the thermodynamic activity of water in the solutions. Bunge et al. (2012) reasoned that BE steady-state fluxes can therefore be explained by the effects of BE-water solutions on skin hydration status. While the data support this hypothesis, no direct evidence was provided linking BE exposure and skin hydration.

Human skin permeability measurements for HPA are, to our knowledge, lacking in the peer reviewed literature. Dermal exposure to HPA may occur during its manufacture, transportation and industrial use. Dedicated systems designed to handle HPA during loading and unloading procedures limit the risk of exposure to spills or leaks during transportation (SIDS, 2004). Nevertheless, moderate systemic toxicity of this chemical, which is also known to be a severe skin irritant, warrants the study of its dermal absorption potential. Therefore one goal of the present study was to provide these data for dermal risk assessment purposes.

HPA is not used in aqueous solutions in the industrial setting, but the miscibility of this chemical in water presented an opportunity to investigate its skin permeation in a manner comparable with the well-studied water miscible chemical BE. Steady-state fluxes and lag times of HPA in both heat separated human epidermal membranes and silicone rubber membranes were undertaken over the full range of HPA-H₂O concentrations. Thermodynamic activities of HPA and H₂O in aqueous solutions of HPA were measured to

gain knowledge of the driving force for permeation and to gain insight into the effect of H₂O activity on skin permeation. A further set of permeation experiments was designed such that HPA thermodynamic activity could be held constant, while H₂O activity was varied from about 0.8 to 1. Finally, water uptake into desiccated human stratum corneum was measured following incubation in aqueous HPA solutions. Results presented here offer incontrovertible evidence that stratum corneum becomes dehydrated with increasing HPA concentrations, and that this dehydration substantially increases the barrier property of the skin to this chemical.

2. Methods

2.1. Materials

Fresh full thickness human skin samples from Caucasian female (age range: 32–62 y) nonmalignant mammoplasties were obtained on the day of surgery from the West Virginia University Tissue Bank. Skin was submersed in 60 °C buffer for 60 s. Epidermis was teased from underlying tissue with cotton swabs, floated onto buffer + 10% glycerol, and stored frozen (–85 °C) until use. Medical grade silicone rubber sheeting (thickness: 0.020 in. and 0.040 in.) was purchased from Bioplexus.

Commercial grade HPA (CAS: 25584-83-2) was purchased from Monomer-Polymer & Dajac Laboratories, Inc. (Lot number 22-49-4: reported purity 97.5%; methyl ethyl hydroquinone added (reported 217 ppm) to inhibit spontaneous polymerization). Typical commercial formulations of HPA consist of two isomers containing approximately 75–80% 2-hydroxypropyl acrylate and 20–25% 1-methyl-2-hydroxyethyl acrylate (SIDS, 2005). In preliminary studies, there were no discernible differences in the permeability of the 2 isomers. Because of this observation, and because this product is marketed as “HPA”, in all studies described here the sum of the isomers was taken as the HPA quantity.

Tritiated water (specific activity, 1 mCi/g (37 MBq/g)) was purchased from Moravek Biochemicals. Hanks balanced salt solution (HBSS) was purchased from Gibco-Invitrogen Corporation. Soluene 350 (tissue solubilizer) and Ultima Gold (liquid scintillation fluid) came from PerkinElmer. Other chemicals were purchased from Sigma–Aldrich or affiliates and were the highest purity available. Trypsin was type II-S from porcine pancreas. Poly(ethylene glycol) (PEG-1500) had a *MW* range of 1400–1600. Buffer (pH 7.40 @ 37 °C) consisted of 5.96 g HEPES buffer, 0.32 g NaHCO₃, and 0.05 g gentamicin sulfate added to 1000 mL HBSS.

2.2. HPA solutions

All solutions were mixed gravimetrically. HPA-H₂O solutions were mixed to achieve desired mole fractions (x_{HPA}) or volume fractions (ϕ_{HPA}) of HPA. These are defined as:

$$x_{\text{HPA}} = \frac{n_{\text{HPA}}}{n_{\text{HPA}} + n_{\text{H}_2\text{O}}} = \frac{m_{\text{HPA}}/MW_{\text{HPA}}}{(m_{\text{HPA}}/MW_{\text{HPA}}) + (m_{\text{H}_2\text{O}}/MW_{\text{H}_2\text{O}})}, \quad (1)$$

where n is the number of moles, m is mass and MW is molecular weight. The MW of HPA is 130.14; that of H₂O is 18.02.

$$\phi_{\text{HPA}} = \frac{V_{\text{HPA}}}{V_{\text{HPA}} + V_{\text{H}_2\text{O}}} = \frac{m_{\text{HPA}}/\rho_{\text{HPA}}}{(m_{\text{HPA}}/\rho_{\text{HPA}}) + (m_{\text{H}_2\text{O}}/\rho_{\text{H}_2\text{O}})}, \quad (2)$$

where V is volume and ρ is density. The ρ of HPA is 1.045 g/mL (SIDS, 2005) and that of water is 1.000 g/mL.

PEG-1500-H₂O solutions were mixed to achieve desired mass fractions (w_{PEG}), defined as:

$$w_{\text{PEG}} = \frac{m_{\text{PEG}}}{m_{\text{PEG}} + m_{\text{H}_2\text{O}}}. \quad (3)$$

HPA-PEG-1500-H₂O solutions were mixed to achieve desired volume fractions of HPA in solvent consisting of PEG-1500-H₂O solutions of given w_{PEG} :

$$\phi_{\text{HPA}} = \frac{V_{\text{HPA}}}{V_{\text{HPA}} + V_{\text{H}_2\text{O}} + V_{\text{PEG}}} = \frac{m_{\text{HPA}}/\rho_{\text{HPA}}}{(m_{\text{HPA}}/\rho_{\text{HPA}}) + (m_{\text{PEG}}/w_{\text{PEG}}\rho_{\text{PEG}})}, \quad (4)$$

with the density of PEG-1500-H₂O given by (Gonzalez-Tello et al., 1994):

$$\rho_{\text{PEG}} \text{ (g/mL)} = 0.99707 + 0.17441w_{\text{PEG}}. \quad (5)$$

2.3. In vitro permeation studies

Infinite dose permeation studies were undertaken using heat separated human epidermis (HEM) and silicone rubber (SRM) membranes, with HPA-H₂O solutions (ϕ_{HPA} from 0.10 to 1.00) or HPA-PEG-1500-H₂O as donor. Static diffusion cells (Perme-Gear) were used. Exposed surface was 0.64 cm² and receptor volume was 5 mL. A heater/circulator maintained receptor compartment temperature at 37 °C; membrane surface temperatures were 32–33 °C.

Thawed HEM were rinsed in buffer, mounted on cells with dialysis tubing (10 kDa MW cutoff) as membrane support and buffer as receptor, rinsed 3× with water and allowed to equilibrate overnight prior to HPA exposures. Samples from 4 skin donors were used for permeability studies, with 3 replicates from each donor for each tested concentration (Table 2). One additional skin donor contributed 3 replicates each for ϕ_{HPA} of 0.50 and 1.00.

Following overnight equilibration with the outer skin surface open to air, the integrity of the HEM was assessed by measuring transepidermal water flux (AquaFlux AF200, Biox). No membranes were rejected (median: 12.102 g/m²/h; range: 7.246–29.531; $n = 78$). The experiment was initiated ($t = 0$) by the addition of 500 μL of donor solution to each cell. Donor cells were capped. Receptor samples (0.25 mL) were removed and replaced with fresh buffer at 0, 0.5, 1, 2, 3, 4, 6, and 8 h. Donor solution was replaced at 4 h.

Silicone rubber membranes ($n = 3$ per dose) were cut from a single sheet (thickness 0.040 in.). SRM were rinsed with water, mounted on cells, and equilibrated overnight with water

as receptor. Samples (0.25 mL) were removed and replaced with fresh water at 0, 0.5, 1, 2, 3, 4, and 5 h. Donor solution was replaced at 3 h.

HPA in receptor samples was quantified by high performance liquid chromatography (HPLC). Analyses were carried out on an Agilent 1100 HPLC system operating at 22 °C, 0.6 mL/min flow of isocratic mobile phase composed of 10% acetonitrile and 90% H₂O containing 0.01% phosphoric acid. A 10 µL sample was injected onto a Kinetex C18 2.6 µm 100 × 4.6 mm column (Phenomenex). A calibration was carried out prior to each experiment, with adjusted $r^2 > 0.995$. Retention times of the isomers were 5.0 and 5.7 min and their areas were added to calculate concentrations.

Mass absorption per unit area of skin exposure ($m(t)$) was calculated from the measured receptor concentrations, taking into account the amount removed with each sample. Steady-state fluxes (J_{SS}) and lag times (τ) for each membrane were calculated by nonlinear regression (SigmaPlot 11, Systat Software) of the mass absorption data with the 1st 7 terms of the diffusion equation for a homogeneous membrane (Crank, 1975):

$$m(t) = J_{SS}t - J_{SS}\tau - 12 \frac{J_{SS}\tau}{\pi^2} \sum_{n=1}^{\infty} \frac{(-1)^n}{n^2} \exp\left(-n^2\pi^2 \frac{t}{6\tau}\right). \quad (6)$$

For HEM, the 3 replicates from each donor were averaged to obtain the J_{SS} and τ for that donor.

The data from 1 donor were anomalously high—a least 5 standard deviations greater than the mean of the remaining 3 donors. These were excluded from subsequent analysis, but the J_{SS} values are reported in Table 2.

2.4. HPA activity measurements

The thermodynamic activity of HPA (a_{HPA}) in solution was determined by measuring its equilibrium partial pressure relative to that of the pure compound measured at the same defined temperature (Al-Khamis et al., 1982; Frascch et al., 2010). Partial pressures were measured using static headspace gas chromatography (GC). HPA-H₂O solutions (x_{HPA} 0.00 to 1.00) were measured at 32 °C and HPA-PEG-1500-H₂O solutions were measured at room temperature (22–23 °C).

Five hundred µL samples were placed in 10 mL headspace vials. Sample processing was performed with a CombiPal autosampler (CTC Analytics). Samples were equilibrated at the desired temperature for 30 min with intermittent agitation. 100 µL of headspace was injected into the GC injector with split valve off.

The GC was a Varian 3800 with flame ionization detector and trifluoropropyl-methyl polysiloxane capillary column (Restek RTX 200 MS, 30 m length, 0.25 mm ID, 1 µm thickness) with 1 mL/min of He gas flow. The oven temperature program was: initial 60 °C, hold 1 min; ramp 10 °C/min to 160 °C; ramp 50 °C/min to 220 °C. The retention times of the partially unresolved peaks corresponding to the 2 isomers of HPA were 9.6 and 9.7 min. The sum of the areas of the 2 peaks was taken. Activity was calculated as the peak area of

the sample, divided by the peak area of the sample of neat HPA ($x_{\text{HPA}} = 1.00$), measured in triplicate. Three independent determinations were made at each HPA concentration.

2.5. H₂O activity measurements

Water thermodynamic activity ($a_{\text{H}_2\text{O}}$) measurements in HPA-H₂O solutions (x_{HPA} 0.00–1.00) and in HPA-PEG-1500-H₂O were made at room temperature (22–23 °C) with a calibrated relative humidity (RH) sensor (AquaFlux AF200, Biox Systems).

Calibration was performed with saturated aqueous salt solutions. The temperature-corrected RH's of 7 saturated salts (salt + H₂O to form a slurry) were determined by linear interpolation between known quantities tabulated at 5 °C intervals (Greenspan, 1977). The salts and their RH (%) at 20.0 °C were: LiCl (11.3), MgCl (33.1), K₂CO₃ (43.2), NaBr (59.1), NaCl (75.5), KCl (85.1), and K₂SO₄ (97.6). 100 µL of the slurry was placed into the well of a 10 mm sealed sample chamber (Biox). Steady-state RH measurements were recorded after an equilibration period > 10 min. Linearity was excellent ($r^2 > 0.999$) and the slope (AquaFlux reading vs. known RH) was consistent (variance ~2%), but its value was significantly < 1 (mean: 0.607). Steady-state RH measurements were recorded after an equilibration period > 10 min. Water activity was calculated as RH/100%. Three independent determinations were made at each HPA concentration.

2.6. Stratum corneum H₂O uptake measurements

Water uptake into dehydrated human stratum corneum (SC) was measured following incubation in HPA aqueous solutions (0.00–0.99 ϕ_{HPA}). Discs of previously frozen HEM were floated on 0.1% trypsin in buffer and incubated overnight at 37 °C with gentle agitation. Resulting SC discs were rinsed 10 times with water, floated onto Teflon sheets and allowed to dry. They were stored for several days prior to use in a desiccator under laboratory vacuum with freshly regenerated (150 °C for 2 h) silica gel as desiccant. Dehydrated SC discs were weighed to within 0.01 mg and placed individually in glass vials. The SC weights were 1.25 ± 0.22 mg (mean \pm SD, $n = 23$).

HPA-H₂O incubation solutions were mixed to obtain final ϕ_{HPA} of 0.00, 0.25, 0.50, 0.75, 0.90, and 0.99 and an ³H activity of 5 µCi/mL. 2 mL were added to each vial, and SC discs were incubated for 4 h at 32 °C with agitation. The SC were removed, patted dry, rapidly submerged in fresh H₂O, patted dry again, placed into liquid scintillation vials, and dissolved in 1 mL Soluene 350. Radioactivity in SC and incubation solutions was determined by liquid scintillation counting (Packard Tri-Carb). Complete removal of surface water was verified, as rinse water exhibited approximately background radioactivity.

SC samples were used from 3 individual donors, with 3–4 samples total for each HPA concentration tested. SC water weight percent ($w_{\text{H}_2\text{O}}$) was calculated as:

$$w_{\text{H}_2\text{O}} = 100\% \frac{\text{g H}_2\text{O}}{\text{g H}_2\text{O} + \text{g dry SC}} \quad (7)$$

The measured quantity was compared with equilibrium water sorption data reported by Kasting and Barai (2003) using a Frankel-Halsey-Hill (FHH) theoretical isotherm model (Kasting and Barai's eq. (15)). Water activity measurements described above were used in the calculation.

3. Results and discussion

3.1. HPA permeation

Fig. 1 displays representative HPA absorption curves for HEM (top) and SRM (bottom), from which steady-state fluxes and lag times were derived. For HEM, displayed are the means and SD's for 3 discs taken from one skin donor, for $\phi_{\text{HPA}} = 0.25$ and 1.00. For SRM, the means and SD's for 3 membranes are displayed. The solid lines represent best-fit regression curves to the diffusion equation (Eq. (6)), with resulting J_{SS} 's and τ 's. Correlation coefficients (r^2) of the regression for all HEM and SRM data exceeded 0.99. There were no significant differences in the transepidermal water fluxes among any of the HPA concentration groups ($P = 0.121$, analysis of variance (ANOVA) on ranks).

Fig. 2 displays steady-state HPA fluxes across HEM for all HPA concentrations tested. Zero flux at 0 ϕ_{HPA} is assumed, not measured. The data show 3 distinct regions of flux: for ϕ_{HPA} from 0 to 0.25, J_{SS} increases with ϕ_{HPA} . For ϕ_{HPA} from 0.25 to 0.75, J_{SS} remains fairly constant, and for ϕ_{HPA} from 0.75 to 1.00, J_{SS} decreases with ϕ_{HPA} . This type of behavior has been observed previously for the compound 2-butoxyethanol, as discussed by Bunge et al. (2012).

Steady-state HPA fluxes in SRM (thickness 0.040 in.) also display 3 distinct regions (Fig. 3); however the Region III behavior differs in that J_{SS} increases with ϕ_{HPA} . Again, this behavior is similar to that observed with BE (Bunge et al., 2012).

Table 2 summarizes the permeability results for both HEM and SRM. The lag time in HEM is ~2-fold longer with neat HPA as donor than with any other aqueous donor solutions ($P < 0.0005$, ANOVA). None of the other lag times differed significantly from each other. The J_{SS} values for the single skin donor that was deemed an outlier are listed in Table 2. Note that these values, while substantially higher than the others, display the same general 3-region behavior as the others. Inclusion of these values would in no way alter the conclusions drawn from these data.

3.2. Thermodynamic activities of HPA and H₂O in solution

The HPA-H₂O solutions exhibit non-ideal behavior (Fig. 4). Thermodynamic activities of HPA and H₂O are displayed as functions of x_{HPA} (top) and ϕ_{HPA} (bottom). The solid lines represent spline interpolations between the data points, while dashed lines represent activities that would be expected if the solution was ideal. Distinct departures from ideal solution behavior are observed for both HPA and H₂O.

It is important to recognize that (1) the thermodynamically appropriate metric for concentration is mole fraction, and (2) the driving force for permeation is thermodynamic activity, not concentration (Higuchi, 1960). For ideal solutions, activity is a linear function

of mole fraction (Fig. 4, top, dashed lines). In cases where the MW 's of the 2 components of a binary mixture differ by $\sim 10\%$ or more, activity will not be a linear function of volume fraction or mass fraction, even for ideal solutions (Fig. 4, bottom, dashed lines). For an inert, homogeneous membrane, it is expected that J_{SS} is a linear function of thermodynamic activity. If the solution were ideal, then J_{SS} would also be a linear function of mole fraction, but not volume fraction. Thus, neither HEM (Fig. 2) nor SRM (Fig. 3) J_{SS} 's are linear functions of ϕ_{HPA} over all concentrations.

3.3. HPA steady-state fluxes as functions of HPA activity

Figs. 5 and 6 display HPA steady-state fluxes as functions of HPA activity. For SRM (Fig. 5), J_{SS} is a linear function ($r^2 = 0.99$) of a_{HPA} over all concentrations. For HEM on the other hand, the flux data cannot be explained on the basis of HPA activity alone. Flux was linear ($r^2 = 0.91$) only over a_{HPA} ranging from 0 to 0.35. Between a_{HPA} of 0.5 to 1, J_{SS} diminishes with activity. In fact, if the regression line is extrapolated to a_{HPA} of 1, the corresponding J_{SS} would be ~ 25 -fold the actual, measured quantity. Additional experiments were therefore undertaken to elucidate the mechanism underlying the observation that J_{SS} is not a linear function of a_{HPA} over all concentrations.

For aqueous 2-butoxyethanol (BE) solutions, it was hypothesized that the region of diminished BE flux with increasing BE concentration could be explained by dehydration of the stratum corneum (Bunge et al., 2012). For BE weight fraction of 0.8 and above, a sharp drop in the activity-normalized steady-state flux was observed, which coincided with a decrease in water activity of the solution. A similar situation exists with HPA. Water activity remains close to unity for ϕ_{HPA} up to about 0.75; afterward it drops precipitously to ~ 0 for neat HPA (Fig. 4, bottom). Two sets of experiments were designed to address the hypothesis that skin desiccation can explain the steady-state HPA flux observations.

3.4. HPA steady-state fluxes at constant HPA activity with varying H₂O activity

In the first set, the water activity of the donor solution was modified by the addition of a large-molecular weight polymer, PEG-1500, while HPA activity remained nearly constant (variance 4%). Water activity is diminished in PEG-H₂O solutions with increasing PEG concentrations (Ninni et al., 1999). The effect is greatest with lower-molecular weight PEG's (Ninni et al., 1999), but these may penetrate the skin and so a larger MW (1500) was selected for these studies. Björklund et al. (2010) showed that such PEG-H₂O vehicles could be used to regulate drug transport across skin, and observed a strong correlation between drug flux and water activity in skin but not in silicone membranes.

In the present studies, the aim was to create a set of donor solutions that maintained a constant HPA activity with diminishing H₂O activity. Details of the solution compositions and thermodynamic activities, in addition to the flux data, are presented in Table 3. Because of the high viscosity of these donor solutions, side-by-side diffusion cells (PermeGear) were used to enable mixing of the donor. The PermeGear magnetic drive unit was incapable of stirring magnets placed in the donor cells; therefore the cells were placed on a more powerful stirring unit (Varimag Telesys-tem). Experiments on SRM ($n = 3$ per dosing solution) and HEM ($n = 3-6$ per dosing solution) were undertaken at room temperature (22–

23 °C). SRM used for these studies was 0.020 in. thick (half the thickness of those used for permeability studies without PEG). Fig. 7 displays the steady-state flux results for both HEM (top) and SRM (bottom) as functions of water activity. For both sets of membranes, fluxes are normalized by their values at $\phi_{\text{HPA}} = 0.5$, $w_{\text{PEG}} = 0$ to facilitate comparisons. For HEM, there is an abrupt drop in J_{SS} as $a_{\text{H}_2\text{O}}$ decreases from 0.95 to 0.90. Overall, there is a 4.5-fold reduction in J_{SS} as $a_{\text{H}_2\text{O}}$ decreases from 1.00 to 0.82, with constant a_{HPA} . For SRM, some decrease (1.5-fold) is also observed. It may be, despite efforts to provide adequate mixing of the donor, that a boundary layer of dwindling HPA formed with increasing PEG-1500 concentrations (with accompanying increase in viscosity). Nevertheless, these experiments clearly indicate that J_{SS} in HEM is modulated by the water activity of the donor solution.

3.5. H₂O uptake into stratum corneum incubated in HPA-H₂O solutions

Like all biopolymers, stratum corneum exhibits a water sorption isotherm; that is, the equilibrium water content of the SC is a function of the water activity of its environment. For SC, a small amount of water persists even at very low $a_{\text{H}_2\text{O}}$. Water content remains low over a broad range of $a_{\text{H}_2\text{O}}$, with a large increase as $a_{\text{H}_2\text{O}}$ exceeds ~0.8 (Kasting and Barai, 2003). In the second set of experiments, we measured the water uptake of previously desiccated human stratum corneum following incubation with HPA-H₂O solutions. Fig. 8 displays the results. Stratum corneum water content diminishes with ϕ_{HPA} , and the steepness of the reduction is most pronounced as ϕ_{HPA} exceeds 0.75. If the measured water content is presented as a function of water activity, the results can be compared with steady-state SC sorption isotherms. The inset to Fig. 8 compares our measured SC water content with the predictions of the FHH model described by Kasting and Barai (2003). The dashed line is the line of identity; the solid is the linear regression line. The correlation is excellent ($r^2 = 0.97$) and the slope is 0.87. A slope less than unity would be expected if the incubation period of 4 h was insufficient to achieve full equilibrium.

In the *in vitro* permeation studies undertaken here (and also in the *in vivo* setting), one would expect a water activity gradient to exist across the SC: at the inner surface, in contact with epidermis, water activity would be close to unity, while at the upper surface, equilibrium activity would be the same as that within the donor solution. Dehydration-induced structural alterations in the SC would thus also be expected to exhibit a gradient across its thickness. A 25-fold reduction in activity-normalized flux is thus quite remarkable, considering the thin layer over which the increase in skin barrier is distributed.

3.6. Additional observations

The region of abrupt change in J_{SS} revealed in Fig. 7 corresponds to the same region of $a_{\text{H}_2\text{O}}$ between 0.90 and 0.95 where SC exhibits an abrupt change in sorption behavior. Anderson et al. (1973) observed rapid increases in water uptake at 95% RH ($a_{\text{H}_2\text{O}} = 0.95$) and noted a correspondence to a previously observed transition region in NMR and infrared spectroscopic data (Hansen and Yellin, 1972). Water contained in SC at activities below this region is largely bound as primary water of hydration, plus a secondary, less tightly bound species that nevertheless does not freeze at -50 °C. Only at very high humidity does a freer (more mobile) form of water, yet with decreased mobility relative to bulk water, come into

play. The overall picture has been confirmed by more recent analyses (Kasting and Barai, 2003; Yadav et al., 2007, 2009). This water is associated mostly with corneocytes. In this high hydration state, keratin fibrils are apparently surrounded by a continuous water phase. It could be that this more mobile species forms the basis of a high conductance permeation pathway. According to the analysis of Kasting et al. (2003), the fully hydrated corneocytes are essentially transparent to water flux. The larger solute radius and hydrodynamic hindrance would modify the result somewhat for HPA, and a full analysis is beyond the current scope.

The 2–3 fold increase in lag time from neat (undiluted) HPA compared with aqueous HPA (Table 2) suggests an alteration of the permeation pathway in the fully desiccated state. Iwai et al. (2013) showed that dehydration organizes SC intercellular lipids in a vertically compressed arrangement. SC drying leads to a compact, dense structure with enhanced barrier properties. The theoretical foundation of a proposed aqueous pore pathway within SC lipids (Mitragotri, 2003) presumes defects or imperfections within lipid bilayers. Imperfections have been identified as aqueous micro-pores created from discontinuities in lipid lamellar organization (Sznitowska et al., 1998). As SC becomes desiccated, the volumes of these pores would diminish, becoming vanishingly small in the fully desiccated state, leading to increased hindrance of hydrophilic solutes. The diminished permeation rate and increased lag time for neat HPA compared with aqueous solutions is consistent with this interpretation.

4. Summary and conclusions

The permeability behavior from neat and aqueous HPA solutions through human epidermis and silicone membranes has been described. For SRM, the observed dependence of J_{SS} on HPA concentration is expected based on the non-ideal nature of aqueous HPA solutions: J_{SS} is a linear function of a_{HPA} (Fig. 5). For HEM on the other hand, J_{SS} increases with HPA thermodynamic activity up to $a_{HPA} \sim 0.35$ (Fig. 6). As a_{HPA} increases further, J_{SS} decreases. We have provided direct evidence of the effect of diminished a_{H_2O} on J_{SS} : at constant a_{HPA} , J_{SS} decreases with diminishing a_{H_2O} (Fig. 7). Additionally, incubation of human SC with aqueous HPA solutions results in substantial changes in the water content of the SC, dependent on the water activity of the solution and consistent with the known SC water sorption isotherm (Fig. 8). These data provide unequivocal evidence of a substantial increase in epidermal barrier function resulting from SC dehydration. It is reasonable to conclude that dehydration-related alterations in the SC are responsible for the observed flux behavior. In particular, the disappearance of mobile free water at activities less than ~ 0.95 may be key to understanding the observations.

References

- Al-Khamis K, Davis SS, Hadgraft J, Mill S. The determination of thermodynamic activity by gas-chromatography head space analysis and its use in studying release rate of drugs from topical preparations. *Int J Pharm.* 1982; 10:25–28.
- Anderson RL, Cassidy JM, Hansen JR, Yellin W. Hydration of stratum corneum. *Biopolymers.* 1973; 12:2789–2802. [PubMed: 4782554]

- Björklund S, Engblom J, Thuresson K, Sparr E. A water gradient can be used to regulate drug transport across skin. *J Control Release*. 2010; 143:191–200. [PubMed: 20074596]
- Bunge AL, Persichetti JM, Payan JP. Explaining skin permeation of 2-butoxyethanol from neat and aqueous solutions. *Int J Pharm*. 2012; 435:50–62. [PubMed: 22330932]
- Crank, J. *The Mathematics of Diffusion*. 2. Clarendon Press; Oxford: 1975. p. 51
- Frasch HF, Zang LY, Barbero AM, Anderson SE. In vitro dermal penetration of 4-chloro-3-methylphenol from commercial metalworking fluid and aqueous vehicles. *J Toxicol Environ Health A*. 2010; 73:1394–1405. [PubMed: 20818538]
- Gonzalez-Tello P, Camacho F, Blaquez G. Density and viscosity of concentrated aqueous solutions of polyethylene glycol. *J Chem Eng Data*. 1994; 39:611–614.
- Greenspan L. Humidity fixed points of binary aqueous solutions. *J Res Natl Bur Stand A*. 1977; 81A:89–96.
- Hansen, JR.; Yellin, W. NMR and infrared spectroscopy studies of stratum corneum hydration. In: Jellinet, HHG., editor. *Water Structure at the Water–Polymer Interface*. Plenum Press; New York: 1972. p. 19-29.
- Higuchi T. Physical chemical analysis of percutaneous absorption process from creams and ointments. *J Soc Cosmet Chem*. 1960; 11:85–97.
- Iwai I, Kunizawa N, Yagi E, Hirao T, Hatta I. Stratum corneum drying drives vertical compression and lipid organization and improves barrier function in vitro. *Acta Derm Venereol*. 2013; 93:138–143. [PubMed: 23165657]
- Johanson G, Fernstrom P. Influence of water on the percutaneous absorption of 2-butoxyethanol in guinea pigs. *Scand J Work Environ Health*. 1988; 14:95–100. [PubMed: 3387964]
- Kasting GB, Barai ND. Equilibrium water sorption in human stratum corneum. *J Pharm Sci*. 2003; 92:1624–1631. [PubMed: 12884249]
- Kasting GB, Barai ND, Wang TF, Nitsche JM. Mobility of water in human stratum corneum. *J Pharm Sci*. 2003; 92:2326–2340. [PubMed: 14603517]
- Mitragotri S. Modeling skin permeability of hydrophilic and hydrophobic solutes based on four permeation pathways. *J Control Release*. 2003; 86:69–92. [PubMed: 12490374]
- Ninni L, Camargo MS, Meirelles AJA. Water activity in poly(ethylene glycol) aqueous solutions. *Thermochim Acta*. 1999; 328:169–176.
- SIDS. [accessed 20.06.13] Initial assessment report. Hydroxypropyl acrylate CAS No: 25584-83-2. OECD Screening Information DataSet. 2005. <http://www.inchem.org/documents/sids/sids/25584832.pdf>
- Sznitowska M, Janicki S, Williams AC. Intracellular or intercellular localization of the polar pathway of penetration across stratum corneum. *J Pharm Sci*. 1998; 87:1109–1114. [PubMed: 9724563]
- Traynor MJ, Wilkinson SC, Williams FM. The influence of water mixtures on the dermal absorption of glycol ethers. *Toxicol Appl Pharmacol*. 2007; 218:128–134. corrigendum 221: 129. [PubMed: 17173944]
- Yadav S, Pinto NG, Kasting GB. Thermodynamics of water interaction with human stratum corneum. I Measurement by isothermal calorimetry. *J Pharm Sci*. 2007; 96:1585–1597. [PubMed: 17238199]
- Yadav S, Wickett RR, Pinto NG, Kasting GB, Thiel SW. Comparative thermodynamic and spectroscopic properties of water interaction with human stratum corneum. *Skin Res Technol*. 2009; 15:172–179. [PubMed: 19622127]

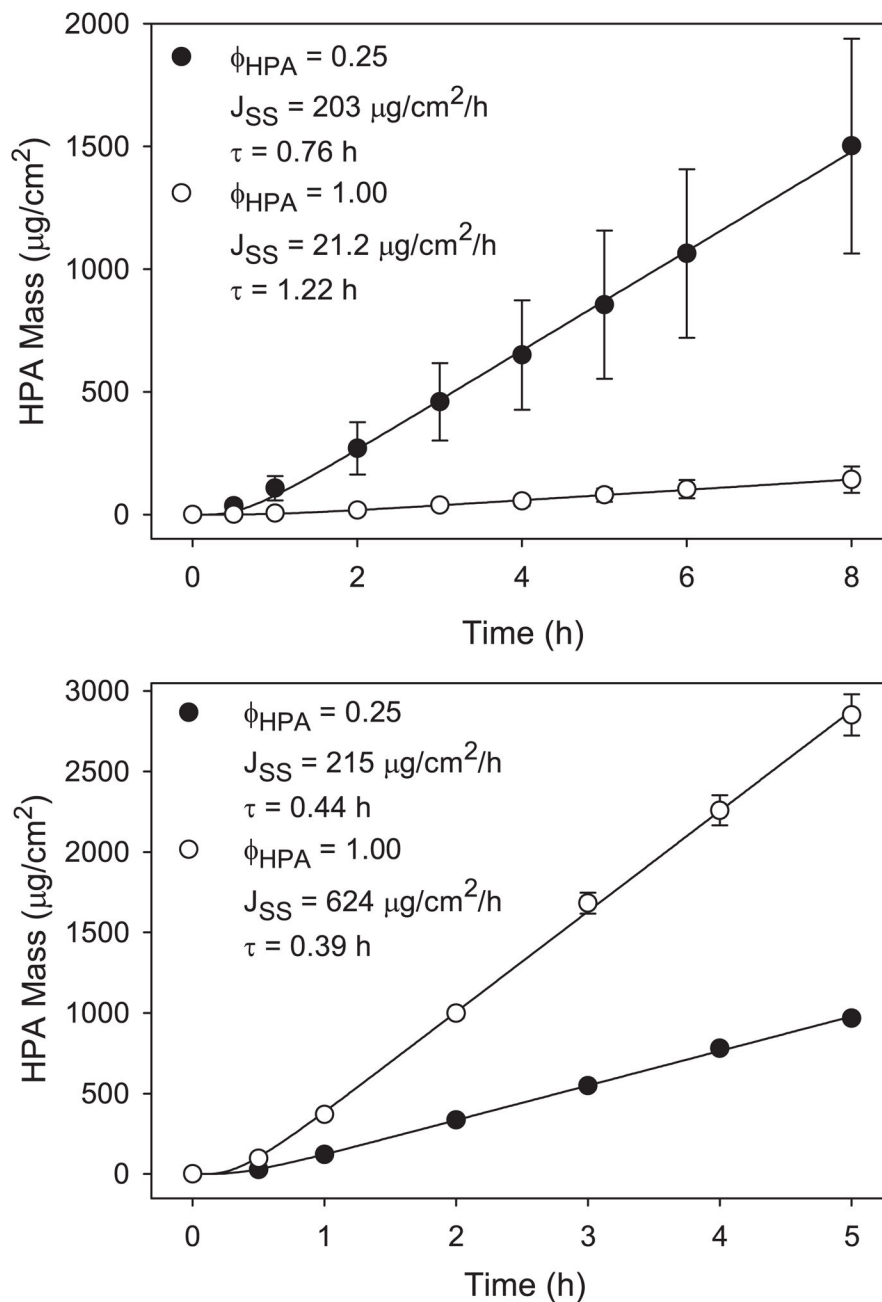


Fig. 1. Representative HPA permeation curves from human epidermis (top) and silicone rubber membranes (bottom), for HPA volume fractions (ϕ_{HPA}) of 0.25 and 1.00. Human epidermis data represent mean \pm SD of 3 replicates from 1 donor; silicone data are mean \pm SD of 3 membranes. Solid lines are best-fit regressions to the diffusion equation (Eq. (6)) with corresponding parameter values for steady state flux (J_{SS}) and lag time (τ).

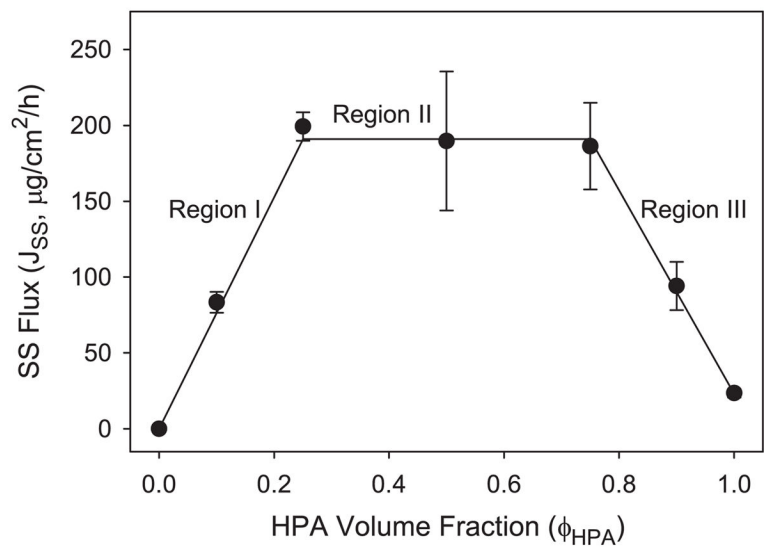


Fig. 2. Steady-state flux of HPA through human epidermis (mean \pm SD, $n = 3-4$ donors) at different HPA volume fractions. Zero flux at 0 concentration is assumed, not measured. Lines (drawn subjectively) represent 3 distinct regions of flux.

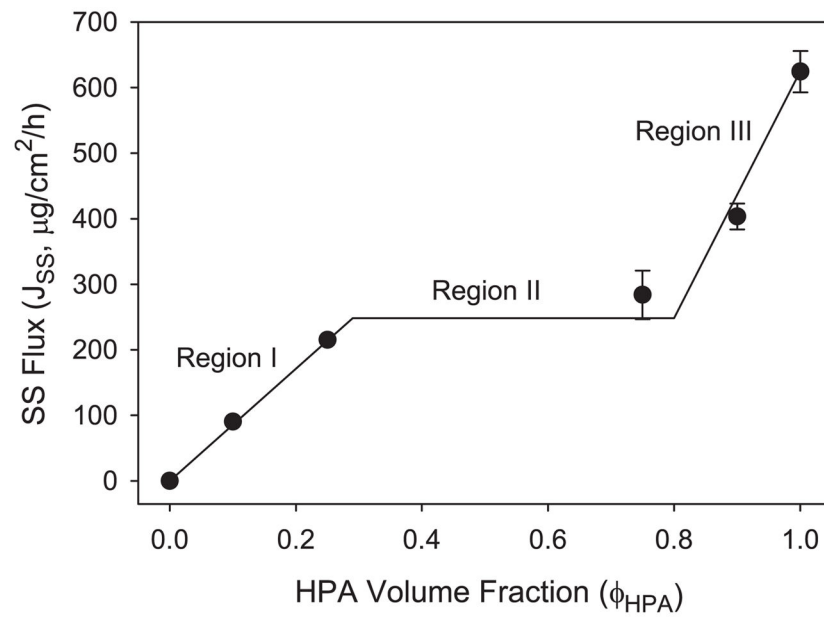


Fig. 3. Steady-state flux of HPA through silicone rubber membranes (mean \pm SD, $n = 3$) at different HPA volume fractions. Zero flux at 0 concentration is assumed, not measured. Lines (drawn subjectively) represent 3 distinct regions of flux.

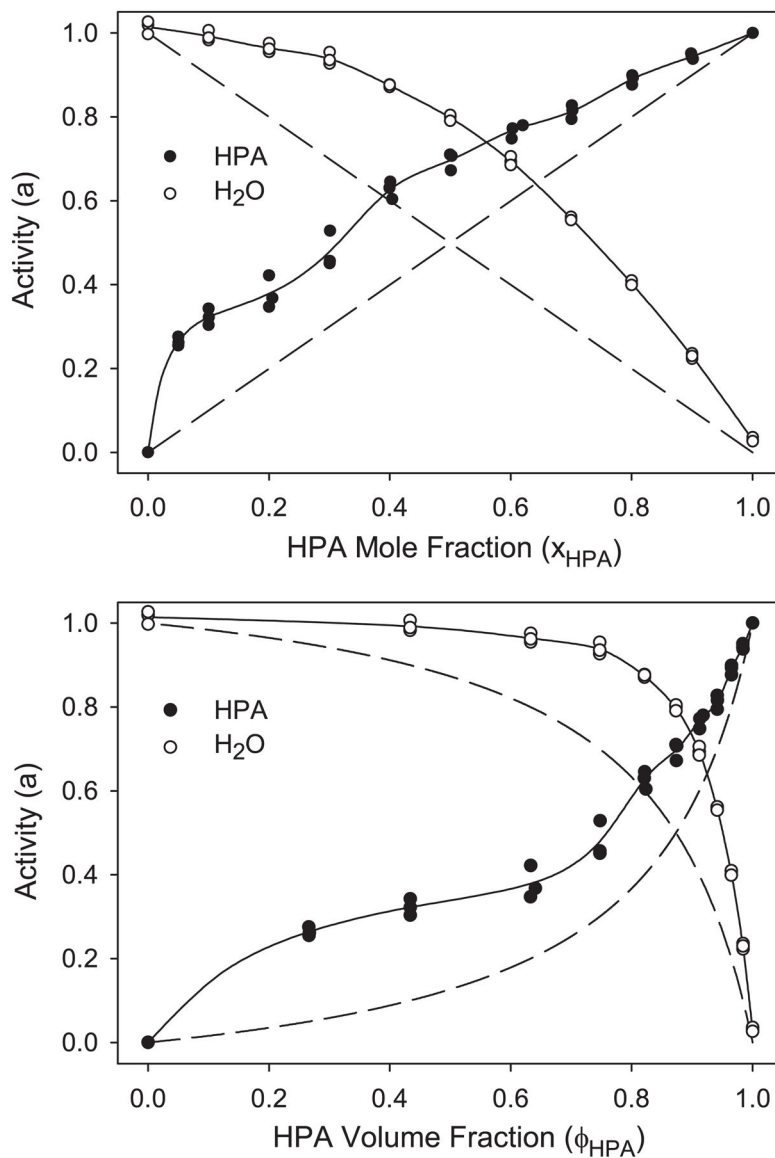


Fig. 4. Thermodynamic activities of HPA and water as functions of mole fraction of HPA (top) and volume fraction of HPA (bottom). Three independent determinations were made for each concentration. Solid lines are spline interpolations between mean values; dashed lines represent ideal solution behavior.

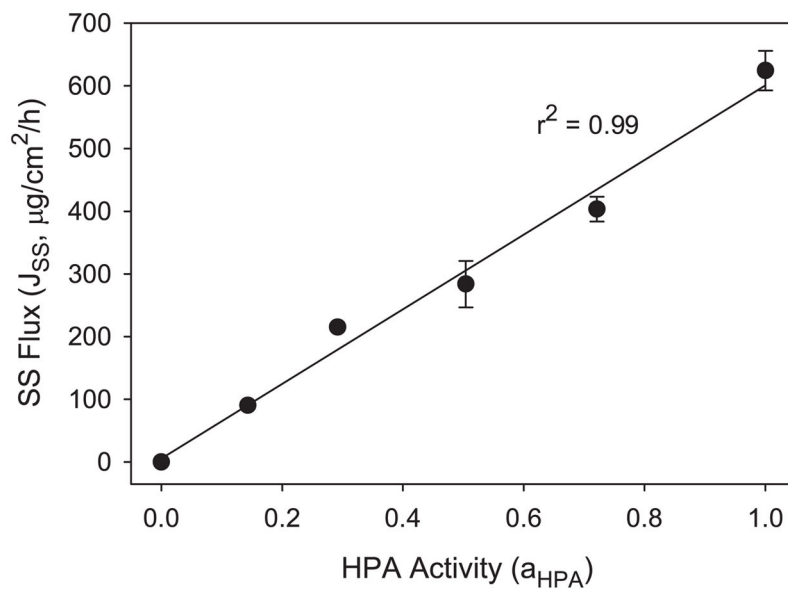


Fig. 5. Steady-state flux through silicone rubber membranes as a function of HPA thermodynamic activity. Zero flux at 0 activity is assumed, not measured. The linear regression line is shown, with resulting correlation coefficient (r^2).

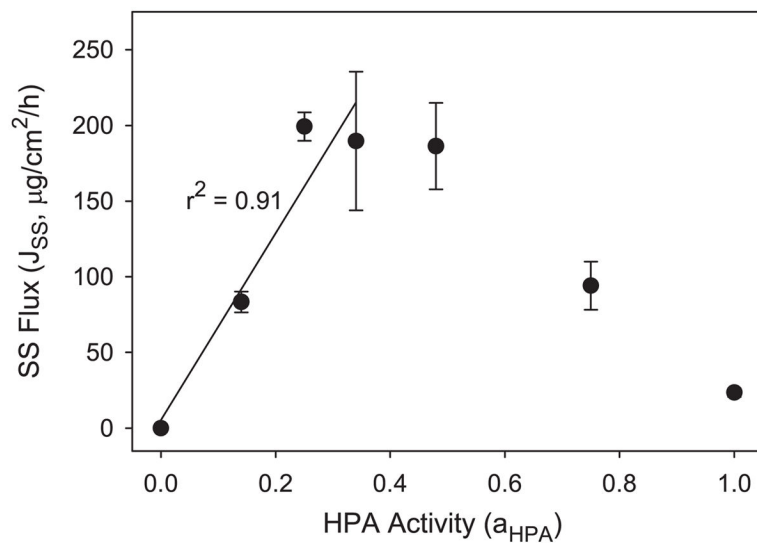


Fig. 6. Steady-state flux of HPA through human epidermis as a function of HPA thermodynamic activity. Zero flux at 0 activity is assumed, not measured. Line is the linear regression of the data from HPA volume fraction 0.00–0.50, with resulting correlation coefficient (r^2).

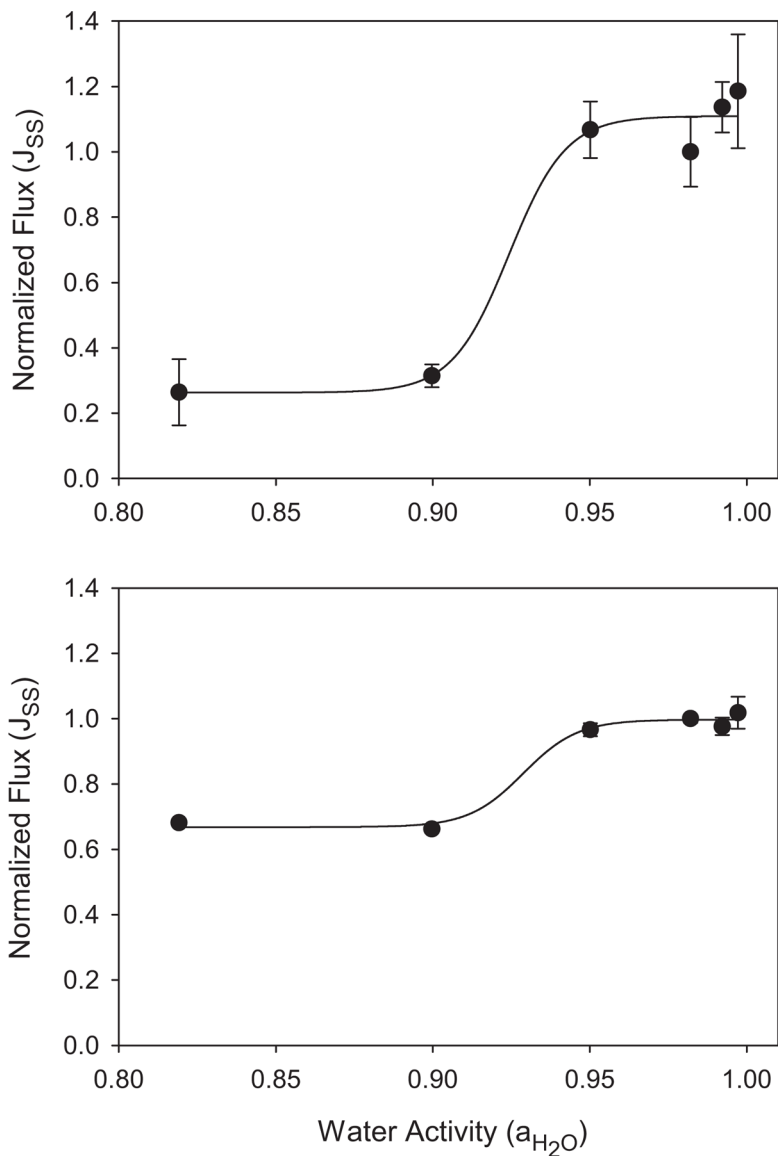


Fig. 7. Normalized steady-state flux of HPA through human epidermal membranes ($n = 3-6$, top) and silicone rubber membranes ($n = 3$, bottom), from donor solutions with constant HPA thermodynamic activity but varying H_2O activity. Shown are mean \pm SD. Fluxes are normalized by their values from 0.50 volume fraction HPA in water. Table 3 gives details of donor composition and activities. Lines are a guide to the eye.

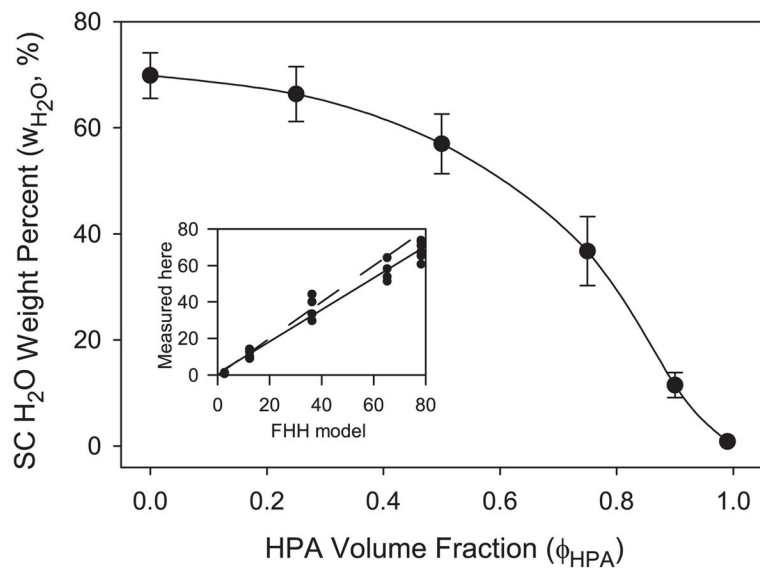


Fig. 8. Water content of isolated, initially desiccated human stratum corneum following 4 h equilibration with HPA-H₂O solutions. Shown are mean \pm SD, $n = 3-4$. Line is spline interpolation. Inset: Comparison of measured data with predictions of the Frankel-Halsey-Hill (FHH) theoretical steady-state isotherm model described by Kasting and Barai (2003). Dashed line is line of identity; solid is the linear regression.

Table 1

Some properties of HPA. CAS: Chemical Abstracts Service Registry Number. Structure of 2 isomers is shown —top: 2-hydroxypropyl acrylate; bottom: 2-hydroxy-1-methylethyl acrylate. $\log K_{ow}$ base 10 logarithm of octanol–water partition coefficient. CSID:55190, <http://www.chemspider.com/Chemical-Structure.55190.html> (accessed May 29, 2013).

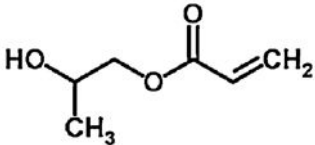
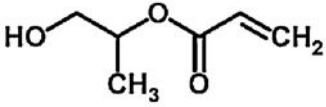
CAS	Formula	Structure	MW	$\log K_{ow}$
				
25584-83-2	C ₆ H ₁₀ O ₃		130.14	0.35
				

Table 2

Donor properties and permeability results. ϕ_{HPA} : volume fraction HPA in water; a_{HPA} : HPA thermodynamic activity; $a_{\text{H}_2\text{O}}$: H_2O thermodynamic activity; J_{SS} : steady-state flux ($\mu\text{g}/\text{cm}^2/\text{h}$, mean \pm SD) across human epidermal membranes (HEM, $n = 3-4$) and silicone rubber membranes (SRM, $n = 3$); outlier: J_{SS} of 1 skin donor excluded from analysis; τ : lag time (h, mean \pm SD).

ϕ_{HPA}	a_{HPA}	$a_{\text{H}_2\text{O}}$	J_{SS} , HEM	J_{SS} , outlier	τ , HEM	J_{SS} , SRM	τ , SRM
0.10	0.14	1.01	83.3 \pm 6.9	217	0.61 \pm 0.24	90.4 \pm 2.7	0.45 \pm 0.03
0.25	0.29	1.00	199 \pm 9	378	0.70 \pm 0.09	215 \pm 4	0.44 \pm 0.03
0.50	0.34	0.99	190 \pm 46	459	0.68 \pm 0.19	–	–
0.75	0.50	0.94	186 \pm 29	414	0.51 \pm 0.25	284 \pm 37	0.45 \pm 0.02
0.90	0.72	0.73	94.1 \pm 16.0	172	0.47 \pm 0.15	403 \pm 20	0.47 \pm 0.03
1.00	1.00	0.03	23.5 \pm 2.9	63.8	1.40 \pm 0.37	624 \pm 32	0.39 \pm 0.03

Donor composition, thermodynamic activities and fluxes for results presented in Fig. 7. w_{PEG} : weight fraction of PEG-1500 in water used as solvent; ϕ_{HPA} : volume fraction of HPA; a_{HPA} : HPA thermodynamic activity; $a_{\text{H}_2\text{O}}$: H₂O thermodynamic activity; J_{SS} : steady-state flux ($\mu\text{g}/\text{cm}^2/\text{h}$, mean \pm SD) across HEM ($n = 3-6$) and SRM ($n = 3$). Studies were undertaken at room temperature ($22-23$ °C).

Table 3

w_{PEG}	ϕ_{HPA}	a_{HPA}	$a_{\text{H}_2\text{O}}$	J_{SS} , HEM	J_{SS} , SRM
0.00	0.50	0.28	0.98	79.8 ± 8.5	497 ± 6
0.10	0.38	0.27	1.00	94.6 ± 13.9	506 ± 24
0.20	0.31	0.30	0.99	90.7 ± 6.2	485 ± 13
0.35	0.35	0.28	0.95	85.2 ± 6.9	480 ± 10
0.50	0.17	0.29	0.90	25.1 ± 2.8	329 ± 3
0.65	0.22	0.28	0.82	21.1 ± 8.1	339 ± 0